ANALYSIS OF A PULSED CORONA CIRCUIT

R. Korzekwa (MS-H851) and L. Rosocha (MS-E526)
Los Alamos National Laboratory
P.O. Box 1663, Los Alamos, NM 87545

M. Grothaus
Southwest Research Institute
6220 Culebra Road, San Antonio, TX 78238

Abstract

A fast risetime pulsed corona reactor has been developed to investigate the treatment of polluted gaseous effluents. The pulsed high-voltage circuit used to drive the coaxial reactor tube consists of a controllable constant current power supply, a storage capacitance, a self-breaking spark gap, and fast current/voltage diagnostics. The circuit design is coaxial from the storage capacitor (a length of 50 Ω cable) to the reactor tube (a coaxial wire-tube geometry) to minimize the circuit inductance. Using a high-pressure hydrogen spark gap, the apparatus achieved a risetime of approximately 2 ns. The length of the applied pulse was altered by using different lengths of storage capacitor cable. A minimum pulse width was achieved by using a matching 50 Ω load placed before the reactor tube, which produced a square pulse with a width of 10 ns at the input to the reactor tube. The driving circuit and corona load were simulated using a simple time-varying resistance to represent the corona discharge. The resulting waveforms are compared with those obtained experimentally. The simulation results were also used to verify the integrity of the fast-pulse measurements. Finally, experimentally obtained results are presented on the effect of the corona pulse width on the efficiency of NO decomposition in nitrogen.

I. INTRODUCTION

Nonthermal plasmas, of which the pulsed corona discharge is one type, have been extensively investigated [1-3]. A nonthermal plasma can be produced at atmospheric pressure by a transient electrical discharge in which high-energy electrons are created in a low temperature background gas. Pulsed corona discharge systems achieve this by applying a positive high-voltage pulse to a field enhancing wire in the center of a metal tube. A pulsed power circuit that is commonly used to drive the corona discharge is a series resonant circuit composed of a storage capacitor, a switch (typically a spark gap), series inductance (usually the stray inductance of the circuit geometry), and the load capacitance of the reactor tube. In this type of circuit the energy in the storage capacitor is resonantly transferred to the capacitance of the reactor tube by the switch through the series inductance, referred to as resonant energy transfer. A corona discharge, which can be represented as a lumped time varying resistance, occurs when the breakdown voltage of the gas in the tube is reached.

A commercially available software package was used to simulate the circuit, producing current and voltages versus time, with and without a corona discharge. These current and voltage waveforms are compared with those obtained experimentally. From these results the effect of a pulsed corona discharge on the series resonant driving circuit is described.

II. EXPERIMENTAL APPARATUS

The pulsed corona apparatus consists of a constant-current power supply, a control module, the pulse forming circuit components, the reactor tube, and electrical diagnostics. The capacitor charging constant current power supply (Electronic Measurements, Inc., Model 500A) is capable of charging the storage capacitor to 40 kV at a rate of 500J/s. A control module was constructed to control the charging cycle of the power supply. The control module sets the repetition frequency and the on-time of the power supply. A small series resistor is required to protect the power supply from voltage reversals. A 120 cm length of RG-217 coaxial cable was used as the storage capacitance. A coaxial high-pressure hydrogen-filled spark gap was placed in series between the storage capacitance and the rest of the circuit and was used in a self-breaking mode. An inductance, much larger than the stray inductance in the circuit, was placed in series between the spark gap and the reactor tube to establish a known value of series circuit inductance. High-voltage probes (Tektronix, model P6015A) were used to measure the voltages on the storage capacitor, V_S, and the reactor tube, V_R. A low inductance current viewing resistor was built into the outer conductor coaxial housing and was used to measure the reactor tube current, I_R.

The reactor tube was constructed using stainless steel and Teflon^{TM} for the components exposed to the reactive chemical species in the gas flow. The insulating gas manifolds contained the coaxial high-voltage feedthrough which provided electrical access to and mechanical support for the corona wire. The coaxial reactor section

0-7803-5498-2/99/$10.00©1999 IEEE.

Report Documentation Page

Form Approved
OMB No. 0704-0188

1. REPORT DATE	2. REPORT TYPE	3. DATES COVERED
JUN 1999	**N/A**	**-**

4. TITLE AND SUBTITLE
Analysis Of A Pulsed Corona Circuit

5a. CONTRACT NUMBER
5b. GRANT NUMBER
5c. PROGRAM ELEMENT NUMBER

6. AUTHOR(S)

5d. PROJECT NUMBER
5e. TASK NUMBER
5f. WORK UNIT NUMBER

7. PERFORMING ORGANIZATION NAME(S) AND ADDRESS(ES)
Los Alamos National Laboratory P.O. Box 1663, Los Alamos, NM 87545

8. PERFORMING ORGANIZATION REPORT NUMBER

9. SPONSORING/MONITORING AGENCY NAME(S) AND ADDRESS(ES)

10. SPONSOR/MONITOR’S ACRONYM(S)

11. SPONSOR/MONITOR’S REPORT NUMBER(S)

12. DISTRIBUTION/AVAILABILITY STATEMENT
Approved for public release, distribution unlimited

13. SUPPLEMENTARY NOTES
See also ADM002371. 2013 IEEE Pulsed Power Conference, Digest of Technical Papers 1976-2013, and Abstracts of the 2013 IEEE International Conference on Plasma Science. Held in San Francisco, CA on 16-21 June 2013. U.S. Government or Federal Purpose Rights License.

14. ABSTRACT
A fast risetime pulsed corona reactor has been developed to investigate the treatment of polluted gaseous effluents. The pulsed high-voltage circuit used to drive the coaxial reactor tube consists of a controllable constant current power supply, a storage capacitance, a selfbreaking spark gap, and fast current/voltage diagnostics. The circuit design is coaxial from the storage capacitor (a length of 50 Q cable) to the reactor tube (a coaxial wiretube geometry) to minimize the circuit inductance. Using a high-pressure hydrogen spark gap, the apparatus achieved a risetime of approximately 2 ns. The length of the applied pulse was altered by using different lengths of storage capacitor cable. A minimum pulse width was achieved by using a matching 50 Q load placed before the reactor tube, which produced a square pulse with a width of 10 ns at the input to the reactor tube. The driving circuit and corona load were simulated using a simple time-varying resistance to represent the corona discharge. The resulting waveforms are compared with those obtained experimentally. The simulation results were also used to verify the integrity of the fast-pulse measurements. Finally, experimentally obtained results are presented on the effect of the corona pulse width on the efficiency of NO decomposition in nitrogen.

15. SUBJECT TERMS

16. SECURITY CLASSIFICATION OF:			17. LIMITATION OF ABSTRACT	18. NUMBER OF PAGES	19a. NAME OF RESPONSIBLE PERSON
a. REPORT	b. ABSTRACT	c. THIS PAGE			
unclassified	**unclassified**	**unclassified**	**SAR**	**4**	

Standard Form 298 (Rev. 8-98)
Prescribed by ANSI Std Z39-18

was composed of a 2.4 cm inner diameter, 90 cm long stainless steel tube with a 500 μm diameter stainless steel wire. A dry nitrogen flow of 2 l/min in the reactor tube was used to provide a consistent gas medium for all of the measurements.

The equivalent circuit for the pulsed corona system is shown Fig. 1. The high-voltage constant current power supply was modified to reduce the internal output capacitance, C_O, from 230 pF to 24 pF enabling better energy efficiency when charging and discharging the storage capacitor. The resistor $R_P = 1700\ \Omega$ was used to protect the power supply. The combination of the coaxial cable and the stray capacitance in the coaxial high-voltage connections, C_S, is 145 pF. The energy stored in C_S is transferred to the reactor tube by the spark gap switch through the series inductance, $L = 2\ \mu H$. The stray capacitance, C_d, of the coaxial diagnostics section, which contains the current and voltage probes, was measured to be 8 pF. The resistor $R_{CVR} = 0.05\ \Omega$ was used to measured I_R. The measured reactor tube capacitance, C_R, was 19 pF. The discharge resistance is represented by a time varying resistance, R_R.

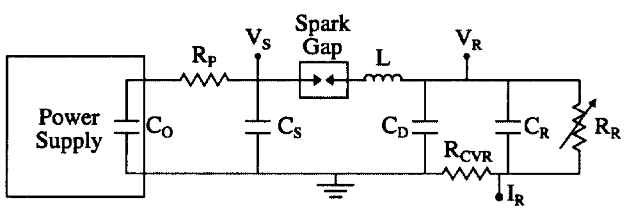

Figure 1. The series resonant high-voltage pulse circuit.

III. CIRCUIT SIMULATION

The SPICE based circuit simulation code used was ICAP/4 Lite™ written by Intusoft, Inc. [4]. The circuit model is shown in Fig. 2 which is the equivalent circuit of Fig. 1 with R_{SG} representing the spark gap and R_{VARES} representing R_R. Before t=0, C_O and C_S are charged to the initial voltage. The spark gap is modeled as a switch that is assumed to close at t=0 and is equal to R_{SG} during the conduction phase. The corona discharge is modeled by a time varying resistance, R_{VARES}, the value of which is determined by a voltage pulse giving the relationship $R_{VARES} = R_O{*}\exp(2{*}V2)$, where $R_O = 1\ \Omega$ is the nominal resistance and V2 is the controlling exponential pulse voltage. From the measured corona resistance versus time the pulsed voltage parameters of V2 can be derived.

IV. COMPARISON OF RESULTS

The pulsed corona reactor experiment was operated close to the onset voltage required to produce a corona discharge in the reactor tube by adjusting the spark gap electrode spacing which sets the switch breakdown voltage. Due to the small variation in breakdown voltage of the spark gap and the statistical time lag associated with the corona initiation process, a variable time delay, τ_D, occurs from shot-to-shot between the onset of the corona discharge and the closing of the spark gap. Using these waveforms, the current and voltage characteristics of the corona discharge alone can be obtained since the corona discharge is now separate from the resonant energy transfer process. The resulting discharge resistance, R_R, can be modeled using R_{VARES} with the appropriate V2 pulse parameters..

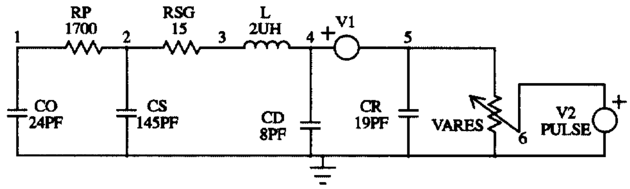

Figure 2. A the series resonant circuit used by the simulation software package.

The experimentally measured waveforms (I_R, V_R, and V_S) and simulated waveforms (I{V1}, V_{N5}, and V_{N2}) of the series resonant circuit are shown in Fig. 3. In Fig. 3, a) compares the currents versus time, b) compares the reactor voltages versus time, and c) compares the voltages across C_S versus time. The resonant energy transfer can be seen within the first microsecond. The current waveform produced by this resonant circuit is an exponentially decaying oscillation seen in Fig. 3a. The reactor voltage waveform, Fig. 3b, is also an exponentially decaying oscillation but is centered around the final charging voltage equal to $V_{CO}C_L/C_T$. When C_S>>C_L, the waveform of the voltage across C_S, Fig. 3c, has small oscillations that are also centered around the final voltage but with a starting voltage equal to V_{CO}.

When a corona discharge is initiated and τ_D is large enough, both the resonant energy transfer and corona discharge electrical characteristics can be recorded separately, as shown in Fig. 3 after 1 microsecond. Along with the resonant energy transfer early in time, there is an additional current and voltage associated with the corona discharge, seen at approximately 1100 ns after the beginning of the waveforms. The current and voltage versus time of the corona discharge are of particular interest since the time varying resistance obtained from V_R/I_R during this time can be used to determine the parameters necessary to create a similar time varying resistance in the circuit simulation model.

The resulting corona resistance versus time of the corona discharge portion of the experimental waveform in Fig. 3d can be found from the ratio of the current and voltage. From this, the simulation voltage pulse parameters of V2 used to control the variable resistor were derived where $\tau_D = 1090$ ns. Using the double-exponential dependence of V2 to control R_{VARES} produces the simulated resistance versus time seen in Fig. 3. There

is good agreement between experimental versus simulated current, voltage, and resistive waveforms.

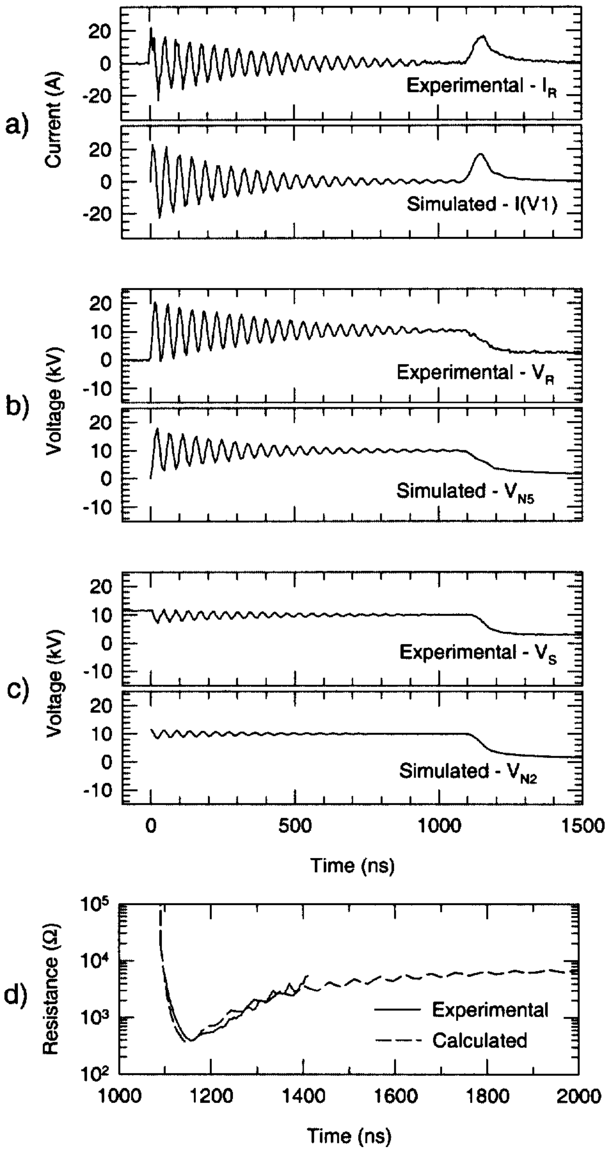

Figure 3. The currents and voltages versus time showing the separation of the resonant energy transfer process from the corona discharge in which the experimental and simulated waveforms are compared where a) is the reactor current, b) is the reactor voltage, and c) is the voltage across the storage capacitor, and d) is the corona discharge resistance.

As τ_D is reduced, experimentally obtained current and voltage waveforms show the effect of the corona discharge occurring during the resonant transfer process. The experimentally obtained waveforms with a very small delay, $\tau_D \sim 35$ ns, are shown in Fig. 4. These waveforms represent what is more typically observed in a pulsed corona circuit under normal operating conditions. With the appropriate reduction in delay to $\tau_D \sim 35$ ns, the simulated waveforms again show good agreement with the experimental waveforms.

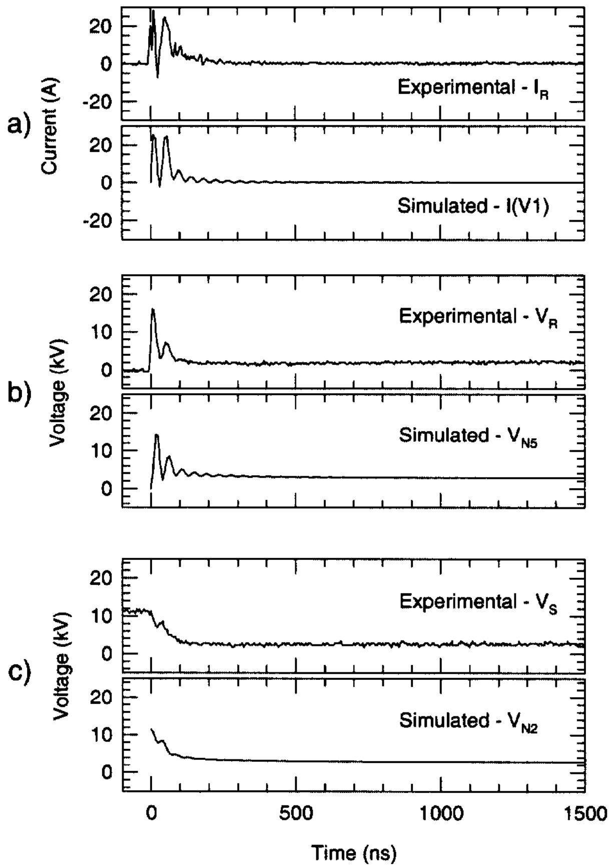

Figure 4. The currents and voltages versus time showing the corona discharge occurring in the beginning of the resonant energy transfer process in which the experimental and simulated waveforms are compared where a) is the reactor current, b) is the reactor voltage, and c) is the voltage across the storage capacitor.

V. TRANSMISSION LINE REACTOR

In Fig. 5, the circuit for the transmission line driven pulsed corona reactor is shown. The storage cable has a delay of 5 ns and an impedance of 50 Ω. The pulsed corona tube can be represented as a coaxial transmission lin which has a delay of 3 ns and an impedance of 235 Ω. The 50Ω line (charged to 30 kV) is matched into a 50 Ω load immediately before the corona tube to eliminate any reflections. The spark gap is modeled as a time varying resistance and a small stray inductance. The pulsed corona discharge is also modeled as a time varying resistance similar to the series resonant pulsed corona circuit.

Figure 6 shows the experimentally obtained waveforms for the current and voltage in the transmission line driven

pulsed corona reactor. The simulated waveforms are also shown and in Fig. 6 which compare favorably to the experimental results. The importance of using the transmission line driven reactor is to limit the corona pulse to a very short time (10 ns). As seen in Fig. 7, the decrease of the corona pulse to 10 ns requires a lower energy density (in joules per liter, J/l) in the reactor to remove the NO from the gas stream.

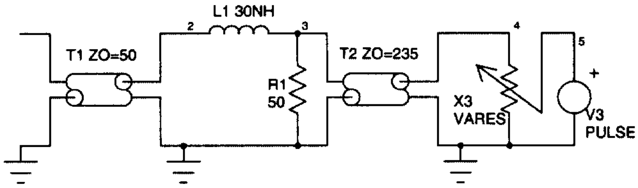

Figure 5. The transmission line driven circuit used by the simulation software package.

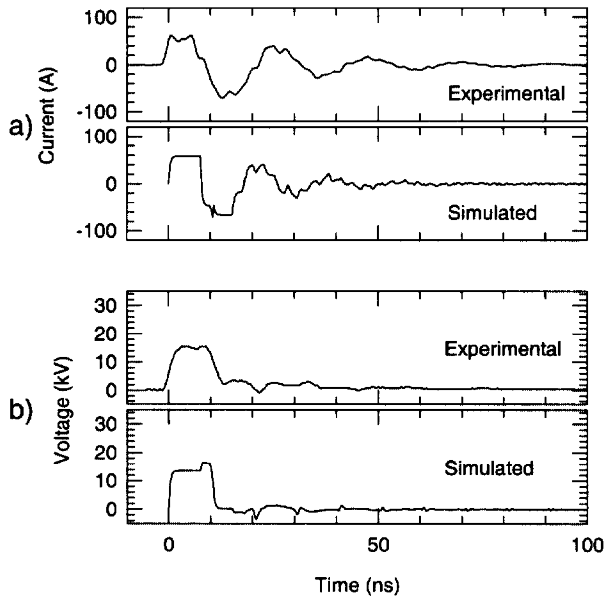

Figure 6. The currents and voltages versus time of the transmission line driven corona discharge in which the experimental and simulated waveforms are compared where a) is the reactor current, and b) is the reactor voltage.

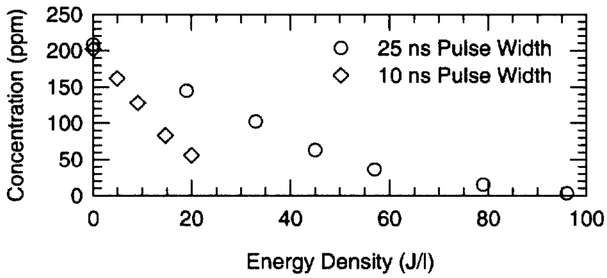

Figure 7. The energy density versus removal for NO in nitrogen for a series resonant and transmission line driven pulsed corona reactor.

VI. SUMMARY

A series resonant and transmission line driven pulsed corona circuit with and without a corona discharge have been modeled using a circuit simulation software package. A comparison of the calculated and simulated current and voltage waveforms with those obtained experimentally has shown that the discharge can be modeled as a separate time varying resistance. Also, for typical current and voltage waveforms of a pulsed corona discharge reactor, the waveform structure is shown to be the combination of oscillations from the series resonant portion of the driving circuit and the overdamped pulse of the corona discharge and not streamer discharge mechanisms such as primary and secondary streamer phenomena.

VII. REFERENCES

[1] B.M. Penetrante and S.E. Schultheis, Editors, Non-Thermal Techniques for Pollution Control, Parts A and B, New York: Springer-Verlag: 1992.

[2] J.S. Chang, P. Lawless, and T. Yamamoto, "Corona Discharge Processes," IEEE Trans. Plasma Sci., vol. **19**, no. 6, Dec., pp. 1152-1166, 1991.

[3] M. Rea and K. Yan, "Evaluation of Pulse Voltage Generators," IEEE Trans. Industry Applications, vol. **31**, no. 3, May/June, pp. 507-512, 1991.

[4] ICAP/4Lite XTRA Circuit Simulation Software, Rev. 95/9, Intusoft, Inc., P.O.Box 710, San Pedro, CA 90733-0710.